Epilepsy & Behavior Reports 14 (2020) 100363

Contents lists available at ScienceDirect

Epilepsy & Behavior Reports

journal homepage: www.elsevier.com/locate/ebcr

Acute modulation of the limbic network with low and high-frequency stimulation of the human fornix

Ganne Chaitanya [a,1], Emilia Toth [a,1], Diana Pizarro [a], Leonidas Iasemidis [b], Teresa A. Murray [b], Kristen Riley [c], Sandipan Pati [a,*]

[a] Epilepsy and Cognitive Neurophysiology Laboratory, Department of Neurology, University of Alabama at Birmingham, Birmingham, AL, USA
[b] Center for Biomedical Engineering and Rehabilitation Science, Louisiana Tech Institute, Ruston, LA, USA
[c] Department of Neurosurgery, University of Alabama at Birmingham, Birmingham, AL, USA

ARTICLE INFO

Article history:
Received 6 February 2020
Received in revised form 25 March 2020
Accepted 26 March 2020
Available online 23 April 2020

Keywords:
Temporal lobe epilepsy
Stimulation
Fornix
Evoked potentials
Excitability
High gamma activation

ABSTRACT

Targeted stimulation of white matter has opened newer perspectives in the field of neuromodulation, towards an attempt to improve memory or as a therapy for epilepsy. Stimulation of the fornix, being a part of the Papez circuit, is likely to modulate the limbic network excitability. However, the stimulation-frequency dependent variability in network excitability is unknown. In the case study, which involved stereo electroencephalographic (SEEG) recording of field potentials in a 48-year old left-handed woman with suspected temporal lobe epilepsy, we demonstrated the network effects of acute low (1 and 10 Hz) and high (50 Hz) frequency electrical stimulation of fornix. Mapping the short-latency evoked responses to forniceal stimulation confirmed the SEEG target localization within the Papez circuit. Low and high-frequency stimulation of the fornix produced opposite effects in the post-stimuli excitability, with the latter causing increased excitability in the limbic network that culminated in a clinical seizure. A distinct spectral peak around 8 Hz confirmed that sensing field potentials from the forniceal white matter is feasible. This is the first case study that provided an insight into how the temporal patterning of forniceal stimulation altered the downstream limbic network excitability.

1. Introduction

Restoring function via targeted modulation of the dysfunctional neural circuits has emerged as a therapeutic option that complements medications in chronic neurological illness. While most neuromodulation therapies have targeted gray matter, stimulation of the white matter "axonal" tracks is an attractive alternative for its ability to modulate a distributed network interconnected to the remote stimulation site [1–3]. Such a stimulation strategy may be desirable in diseases like the temporal lobe epilepsy (TLE), where a widespread network dysfunction extends beyond the seizure focus that contributes to significant comorbidities like memory loss and depression. The fimbria-fornix is a fiber tract comprising of over 1 million myelinated and unmyelinated afferent and efferent axons connecting the hippocampal formation with other limbic and extra limbic structures [4,5]. Functionally, the fiber track (i.e., the fornix) is implicated in the recall of episodic memory, and therefore, has been targeted for deep brain stimulation (DBS) in patients with Alzheimer's disease (AD) and epilepsy.

Interestingly, clinical trials with high-frequency forniceal DBS (130 Hz) failed to improve memory in AD while low-frequency (5 Hz), and patterned stimulation (theta-burst stimulation) showed significant memory improvement in a small cohort with epilepsy [2,4,6]. These contrasting results suggest that increasing (or decreasing) the stimulation frequencies of the fornix, will modulate the excitability of the downstream limbic circuit differently, although an electrophysiological study supporting this hypothesis is lacking. We hypothesized that low and high-frequency stimulation of the fornix would result in distinct spatiotemporal network activation patterns, and the nodes that show a stimulation-induced cortical activation are also likely to show a change in post-stimulation cortical excitability.

2. Methods

2.1. Recruitment and consent

The study was approved by IRB, and written informed consent was obtained to perform research recording from deep brain structures such as the thalamus along with stimulation. Patients were explicitly informed about the risks associated with research implantation, and

* Corresponding author at: Epilepsy and Cognitive Neurophysiology Laboratory, Department of Neurology, University of Alabama at Birmingham, CIRC 312, 1719 6th Avenue South, Birmingham, AL 35294, USA.
E-mail address: spati@uabmc.edu (S. Pati).
[1] Equal contributors.

https://doi.org/10.1016/j.ebr.2020.100363

our group has recently reported the consenting process, accuracy, and safety of thalamic implantation [7]. In the present study, the electrode that was planned to sample the anterior thalamic nuclei missed the target by a 1 mm anteriorly and 3 mm inferiorly and ended in the right anterior fornix (Fig. 1A and B).

2.2. Case description

The study was performed on a 48-year old left-handed woman with drug-resistant focal epilepsy since the age of 41 years. She has 2–3 focal impaired awareness seizures (FIAS)/month and bilateral tonic–clonic seizures once a year. MRI showed right hippocampal sclerosis. However, the video-EEG recording showed interictal and ictal activity outside the right temporal lobe extending to the frontal region. She underwent SEEG exploration for localization of seizures (Natus Quantum, Sampling: 2048 Hz, Natus Medical Incorporated, PMT SEEG electrodes 2 mm contacts with 3.5 mm intercontact spacing). Post-SEEG analysis of seizures confirmed the diagnosis of temporal plus epilepsy with seizures localized to the right hippocampus and a relatively consistent spread to the right superior temporal gyrus.

2.3. Electrical stimulation parameters

During her stay in the monitoring unit, she underwent clinical electrical stimulation (Nicolet® stimulator) to localize seizures and language, followed by research stimulation of the fornix with low (1 Hz and 10 Hz) and high frequencies (50 Hz). Forniceal stimulation was performed when all anti-seizure medications were discontinued to record seizures. Stimulation parameters were: bipolar stimulation (fornix as the cathode, adjacent contact being the anode, biphasic, pulse-width: 300 μs, current: 3 mA, stimulation trials: 60 s for 1 Hz, four trials of 5 s each for 10 Hz and one trial with 50 Hz, inter-trial interval: 3 min). We were unable to repeat the 50 Hz stimulation trial as the stimulation evoked an electroclinic seizure. High-frequency stimulation of fornix resulted in a clinical seizure mimicking habitual spontaneous seizures. Both clinical and research stimulations were performed with the charge-balanced biphasic waveforms. Total charge density per stimulated contact was 17.9 μC/cm^2/phase. Total charge delivered was 0.002 C/cm^2 for 1 Hz stimulation, 0.004 C/cm^2 for 10 Hz stimulation and 0.009 C/cm^2 for 50 Hz stimulation which was well within the recommended safe range of clinical stimulation parameters (defined as a charge density: <30μ C/cm^2/phase and a total charge delivered <29 C/cm^2) [8,9].

2.4. Analyses of stereo EEG

At first, we confirmed the localization of the electrode targets to the fornix and other cortical structures, using a pipeline similar to our previous studies where we coregistered the post-implant CT image with the pre-implant structural MRI using LeadDBS and iElectrodes [10–16]. The electrode target was situated in the right anterior fornix and other targets in limbic circuit were also confirmed (Fig. 1A and B). For SEEG analysis, we performed a visual inspection to pre-select spike free epochs to avoid epileptiform spike confounding the analysis.

2.5. Mapping stimulation-induced neurophysiological markers of connectivity in cortical regions

Single-pulse evoked response (SPES, a.k.a. corticocortical evoked potentials- CCEPs) helps establish the connectivity between the region stimulated and the down-stream propagation of the electrical response along the neuronal pathways. SEEG data of 50 a priori selected channels were preprocessed to remove components with stimulation artifacts and 60 Hz line-noise using 'runica' independent component analysis [17]. Epochs of −250 to 950 ms around the 1 Hz stimulation were parsed on an interleaved along-the-chain bipolar montage with 13 derivations. The evoked potentials (EPs) were detected on band-pass filtered (1–512 Hz, SR:2048 Hz, second-order, Butterworth, zero-phase) data across 3-time epochs: (1) short-latency evoked response (SLEP 0.5 ms–10 ms) [16], (2) A1 (10–50 ms) and (3) A2 (50–200 ms). The epochs were baseline corrected [window: -10 ms to -1 ms prior to stimulation (moving window: 5points, smoothing window: 2.44 ms)], which were later averaged across the 60 stimulations to generate the average response curve (Fig. 2C, D and E). For SLEP, the resultant data was specifically band-passed between 100 and 512 Hz to improve the sensitivity of identifying the SLEP. We considered the response valid only if at least one definitive peak and trough were present on the average response curve depicting the true oscillatory nature of the SLEP. A greater than the median increase in area under the curve (AUC) of the absolute magnitude of the 3 EP-epochs was referred to as SLEP, A1, and A2 [18].

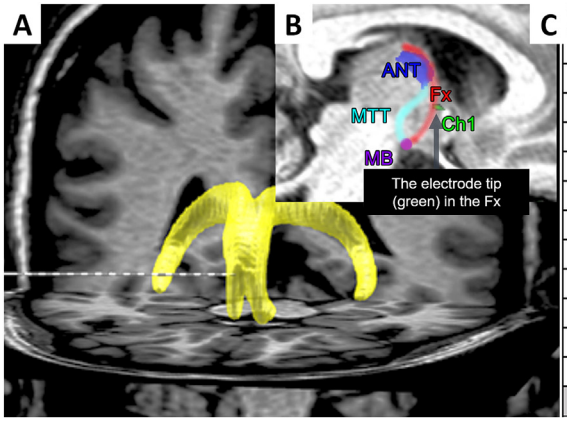

C

Location	Current(mA)	Duration(s)	Frequency	AD/Sz
AntCing	3	5	10Hz & 50Hz	AD
MidCing	3	5	10Hz & 50Hz	-
PostCing	3	5	10Hz & 50Hz	-
OrbF	3	5	10Hz & 50Hz	-
Ins	3	5	10Hz & 50Hz	AD
Ins	3	5	10Hz & 50Hz	AD
TNC	3	5	10Hz & 50Hz	AD
TNC	3	5	10Hz & 50Hz	AD
Amy	3	5	10Hz & 50Hz	AD
HG	3	5	10Hz & 50Hz	AD
Tp	3	5	10Hz & 50Hz	-
Fx	3	5	1Hz, 10Hz	-
Fx	3	5	50Hz	Sz

Fig. 1. Anterior fornix implant: The post-implant computed tomography (CT) image was coregistered with the pre-implant structural MRI using Advanced Normalization Tools [10]. Registration strategies in LeadDBS [13] and iElectrodes [11] were combined to map the electrode trajectories. The cortical regions implanted were confirmed with AAL2 atlas [28] and the thalamic subnuclei with mean histological thalamic atlas. (A) Using the adult template by Brown et al. [12], the electrode target was localized to the fornix. (B) A saggital reconstruction of the forniceal circuit: Anterior nucleus of thalamus ROI of the Morel's atlas and the post implant CT were overlayed on the patient's brain in MRIcro along with the white fiber tracks of fornix, the mammillothalamic tracts and the mamillary body. The electrode tip was found to be located in the anterior fornix (green tip). (C) The stimulation protocol is enumerated: Stimulation of the seizure onset zone (amygdala, hippocampus), superior temporal gyrus and insula at 50 Hz did not result in any seizure but evoked 5–7 s runs of after-discharges. Clinical seizure however was only noted when fornix was stimulated at 50 Hz (AD-After discharge, Sz-seizure, OrbF-orbitofrontal, Acing- anterior cingulate gyrus, MidCing-middle cingulate gyrus, PostCing-posterior cingulate gyrus, Ins-insula, TNC-temporal neocortex consisting of STG and MTG, Amy-amygdala, HG-hippocampal gyrus, Tp-temporal pole, Fx-fornix), MTT- mammillothalamic tract; MB- mammillary body.

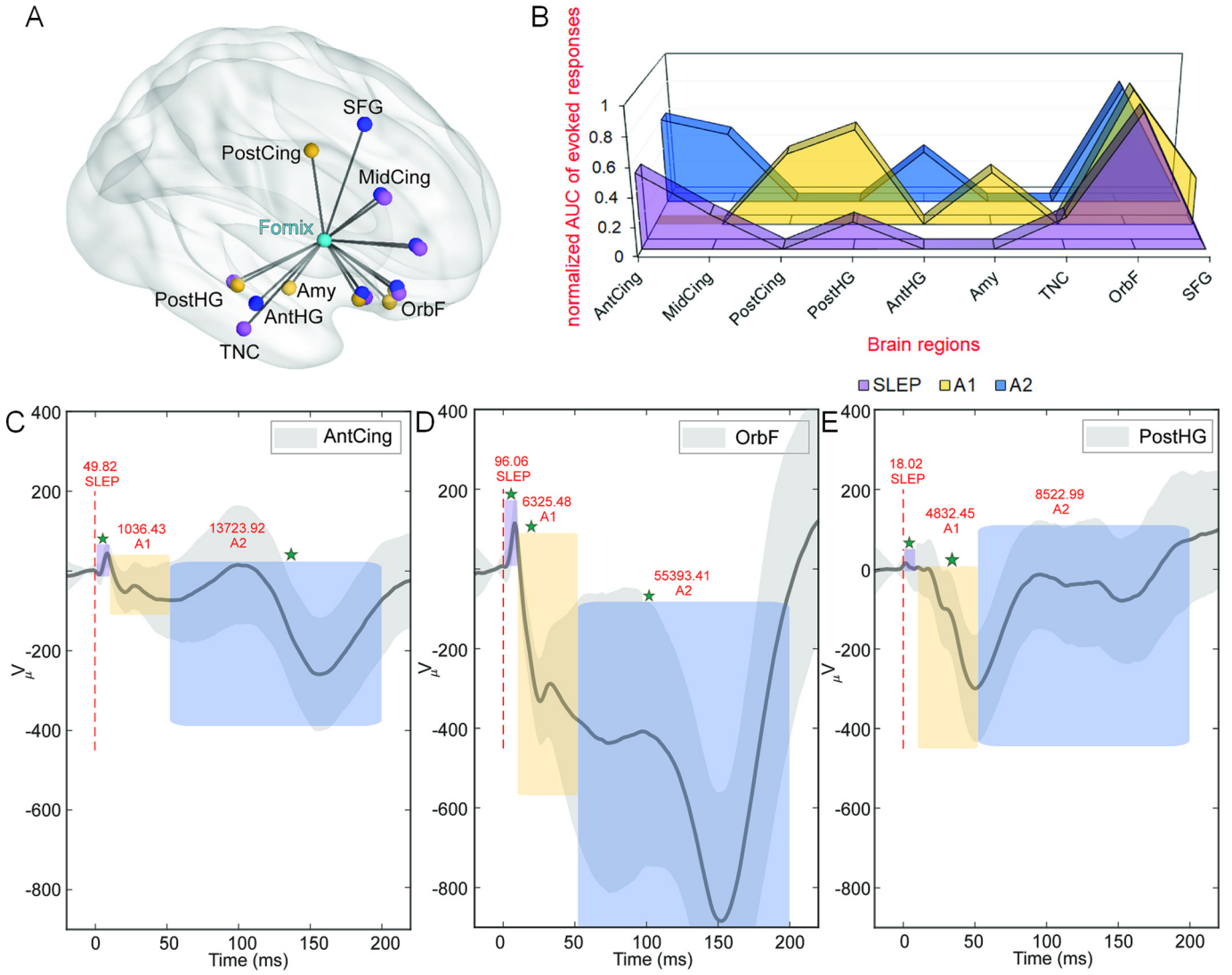

Fig. 2. Evoked potentials: (A) The 3 temporal evoked potentials (EPs) resulting from 1 Hz stimulation of fornix were mapped to the brain [purple nodes: SLEP, yellow nodes: A1 and blue nodes: A2, cyan node: anterior fornix] (BrainNet Viewer: https://www.nitrc.org/projects/bnv/). (B) The 3D line graph shows the AUC of the average response of the 3-temporal EPs i.e., SLEP, A1 and A2. (C,D and E) The EPs had a distinct morphology in 3 temporally distinct phases: SLEP [0.5-10 ms], A1 [10-50ms] and A2 [50-200ms] within specific areas of Papez circuit and fronto-temporal cortices showing these responses. The green star indicates an increase in AUC over the median threshold value. The three example graphs demonstrate the EPs in the AntCing, OrbF and in PostHG respectively. (OrbF: orbitofrontal cortex, AntCing: anterior cingulate cortex, MidCing: middle cingulate cortex, PostCing: posterior cingulate cortex, SFG: Superior frontal gyrus, Amy: amygdala, AntHG: anterior hippocampal gyrus, PostHG: posterior hippocampal gyrus, TNC: temporal neocortex represented by electrodes situated in the middle temporal gyrus).

2.6. Mapping stimulation-induced activation in cortical regions

The change in high gamma activation (HGA: 70-150 Hz) as a proxy of local cortical activation due to increased population neural activity during forniceal stimulation was estimated using Morlet Wavelet decomposition, and the result was baseline normalized [19]. A significant change in stimulation-induced gamma activity was estimated using a one-sample t-test of the pooled and baseline-normalized responses of both low and high-frequency stimulation.

2.7. Estimating changes in intrinsic cortical excitability

Non-oscillatory, 1/f-like activity constituting the background of electrophysiological signals which decays from slower to faster frequencies as per the inverse power law forms an estimate of cortical excitability and was quantified using the slope of a linear regression of the power spectral density [1-150 Hz, Welch's method, Hanning window: 3 s, overlap: 66.67%] fit to the logarithm of x and y axes (i.e., broad-band spectral exponent-β) [20,21]. The changes in intrinsic excitability were measured in the first five seconds epoch after stimulation was terminated. A significant change in post-stimulation excitability was estimated using a one-sample t-test of the pooled and baseline-normalized responses.

2.8. Estimating changes in hippocampal phase amplitude coupling with forniceal stimulation

Phase amplitude coupling (PAC) within the seizure onset zone (i.e., hippocampus), was estimated using complex Morlet wavelet (phases were discretized into 20-degree bins) and was performed on five seconds epochs, each consisting of prestimulation, stimulation, and poststimulation windows [22]. The modulation index derived from the PAC was subjected to t-test between (a) stimulation and prestimulation and (b) poststimulation and prestimulation (Bonferroni corrected P value <.025 was considered significant). Emerging evidence suggests that the phase of slower oscillations modulates the amplitude

of faster ones and has been proposed as a general mechanism of how brain regions coordinate to perform a task.

3. Results

3.1. High-frequency stimulation of the fornix induced clinical seizures

At baseline, a distinct spectral peak around 8 Hz shows that field potentials can be sensed and recorded from the forniceal white matter (Fig. 2A). Both clinical and research stimulations were performed within the recommended safe range (defined as a charge density: <30 μC/cm^2/phase and a total charge delivered <29 C/cm^2). Stimulation of the seizure onset zone (Amygdala, hippocampus), superior temporal gyrus, and insula at 50 Hz did not result in any seizures but evoked 5–7 s runs of after-discharges. However, stimulation of the fornix at 50 Hz resulted in a clinical seizure whose semiology was similar to patient's habitual seizure (Fig. 3B). The semiology consisted of increased palpitation, confusion, and oral automatism.

3.2. Stimulation of the fornix evoked widespread responses within the Papez circuit

Single pulse electrical stimulation (1 Hz) of the anterior fornix elicited 3 temporal evoked potentials (Fig. 2B). Short-latency evoked potentials within 10 ms was noted in posterior hippocampal, anterior-mid cingulate, and orbitofrontal gyri. The A1 evoked potential was the most prominent response and was found along the long axis of the Papez circuit, i.e., along the mid-posterior cingulate, posterior hippocampus, amygdala, the orbitofrontal and temporal neocortex. A2 had a lower amplitude compared to A1 response, mainly in the anterior-mid cingulate, orbitofrontal, and anterior hippocampus.

3.3. Low and high-frequency stimulation of the fornix modulates the excitability of the limbic network differently

The stimulation of the anterior fornix at 1, 10, and 50 Hz elicited specific patterns of cortical activation (high gamma activation) (Fig. 3C) and post-stimulation change in excitability (Fig. 3D). A greater than 1.48 times increase in high gamma activation from the baseline was noted for all stimulation frequencies in the anterior-mid cingulate cortex (high gamma activation: $p = 6.85 \times 10^{-8}$, $t = 7.4$, $df = 26$). Runs of after-discharges were also present with stimulation at 10 and 50 Hz (3 mA) of anterior cingulate, insula, amygdala, hippocampus (Fig. 1). The corresponding change in post-stimulation excitability showed distinct opposite changes, i.e., low frequency stimulation (1 and 10 Hz) mostly decreased excitability within the limbic network while high-frequency stimulation resulted in increased excitability within the limbic network ($p = 3.74 \times 10^{-7}$, $t = 6.7$, $df = 26$).

Stimulation with 50 Hz increased cortical excitability involving broader spatial regions, including the hippocampus, amygdala, temporal

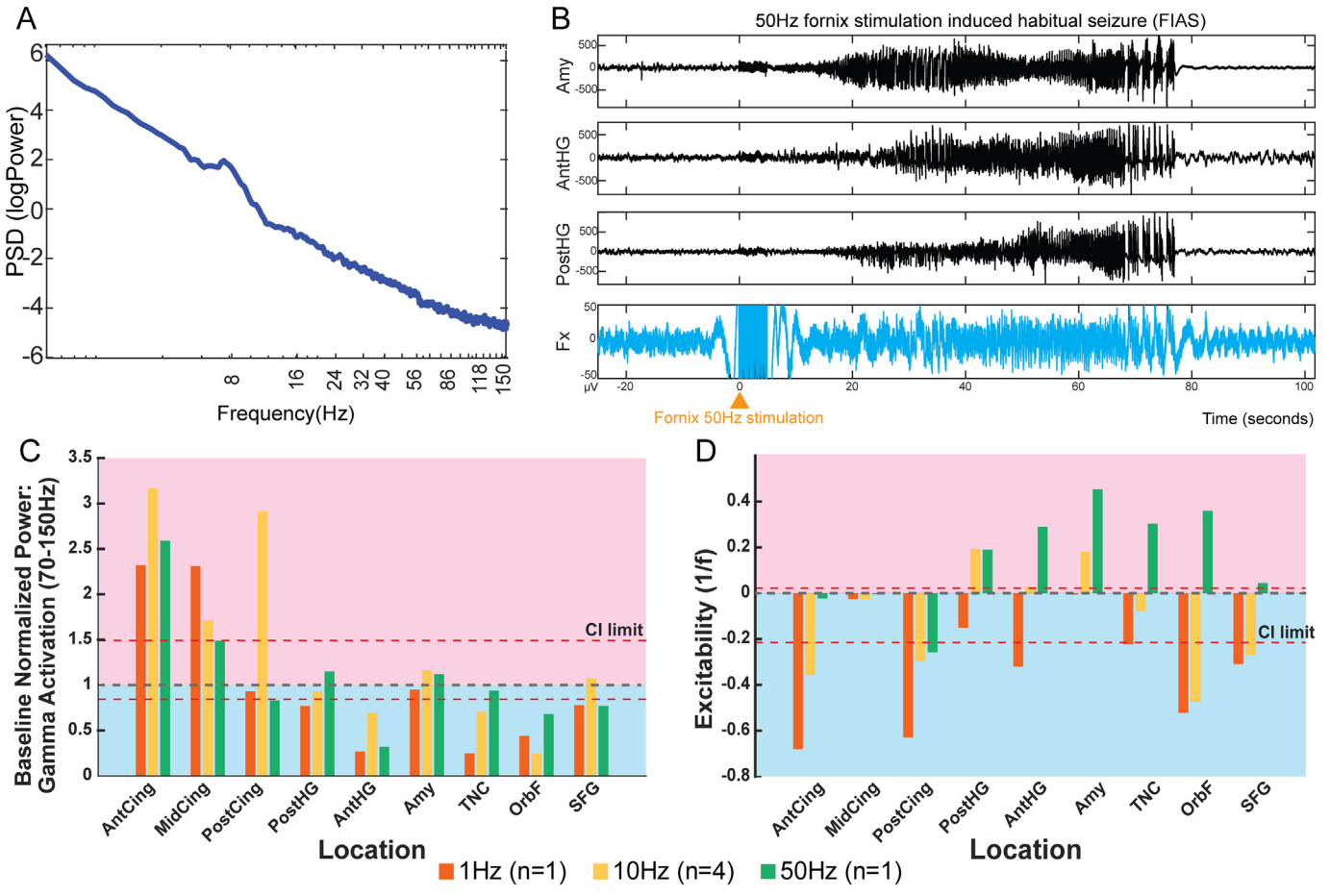

Fig. 3. Gamma activation and cortical excitability: (A) A distinct spectral peak around 8 Hz shows that sensing field potentials from the forniceal white matter is feasible. (B) Stimulation of fornix (Fx) at high frequency (50 Hz) produced a habitual seizure recruiting hippocampus and amygdala. (C) Bar graphs showing baseline normalized gamma activation (HGA: 70-150 Hz) following stimulation with 1 Hz, 10 Hz and 50 Hz of the fornix. The blue hue represents no significant increase in gamma activity over the baseline (gray line) and the red hue indicates gamma activation. (D) The excitability of the cortical regions was estimated using the broad-band spectral exponent β. The blue hue indicates regions showing tissue excitability lower than the baseline and the red hue indicates regions showing tissue excitability greater than the baseline. Stimulation with 50 Hz resulted in increased excitability in regions like those that showed prominent A1 response on CCEPs. A1 and increased excitability were noted in anterior and posterior hippocampus and amygdala.

neocortex, orbitofrontal cortex, and superior frontal gyri. Interestingly, the areas showing increased excitability with 50 Hz were synonymous with the A1 EP network (Fig. 2B).

3.4. Stimulation of fornix altered phase-amplitude (PAC) coupling within the epileptogenic hippocampus

We evaluated the changes in the intra-hippocampal PAC as a function of forniceal stimulation frequencies. During five seconds of stimulation with 10 Hz intra-hippocampal delta-theta/beta coupling was reduced, while with 50 Hz delta-theta/alpha coupling was increased. In the post-stimulation period, increased delta-alpha coupling was noted with 10 Hz and decreased delta-beta coupling with 50 Hz stimulation, respectively (Fig. 4).

4. Discussion and conclusion

DBS to restore memory and learning is critically needed in epilepsy, and a variety of other neurobehavioral illnesses like dementia, and traumatic brain injury. Among different targets, the fimbria-fornix is unique as it is an axonal track which on stimulation recruits remote cortical structures involved in processing memory. In this experimental case study that involved stereotactic EEG (SEEG) recording of field potentials from different nodes within the limbic system, we demonstrate an increase in the excitability of the limbic network culminating in a seizure with higher frequency (50 Hz) stimulation while decreased excitability with lower frequency (1 Hz and 10 Hz) electrical stimulation of the fornix. Overall, we demonstrate that the engagement of the limbic network is a function of stimulation frequencies. The results, albeit limited to acute stimulation, are significant as it highlights that the stimulation parameter of an axonal track can influence ictogenicity, i.e., propensity to induce a seizure which is a neurological paroxysm of gray matter origin. Stimulation induced seizures or after-discharges are undesirable if the goal of the forniceal DBS is to improve memory.

Similar to prior studies [4,23], stimulation of fornix in our research has elicited robust short-latency evoked potentials in cingulate, hippocampus, and orbitofrontal regions that, in conjunction with imaging, confirm the localization of the SEEG electrode. The fornix mainly consists of the outflow fibers from the hippocampal formation, and hence the short-latency in evoked response likely represents antidromic

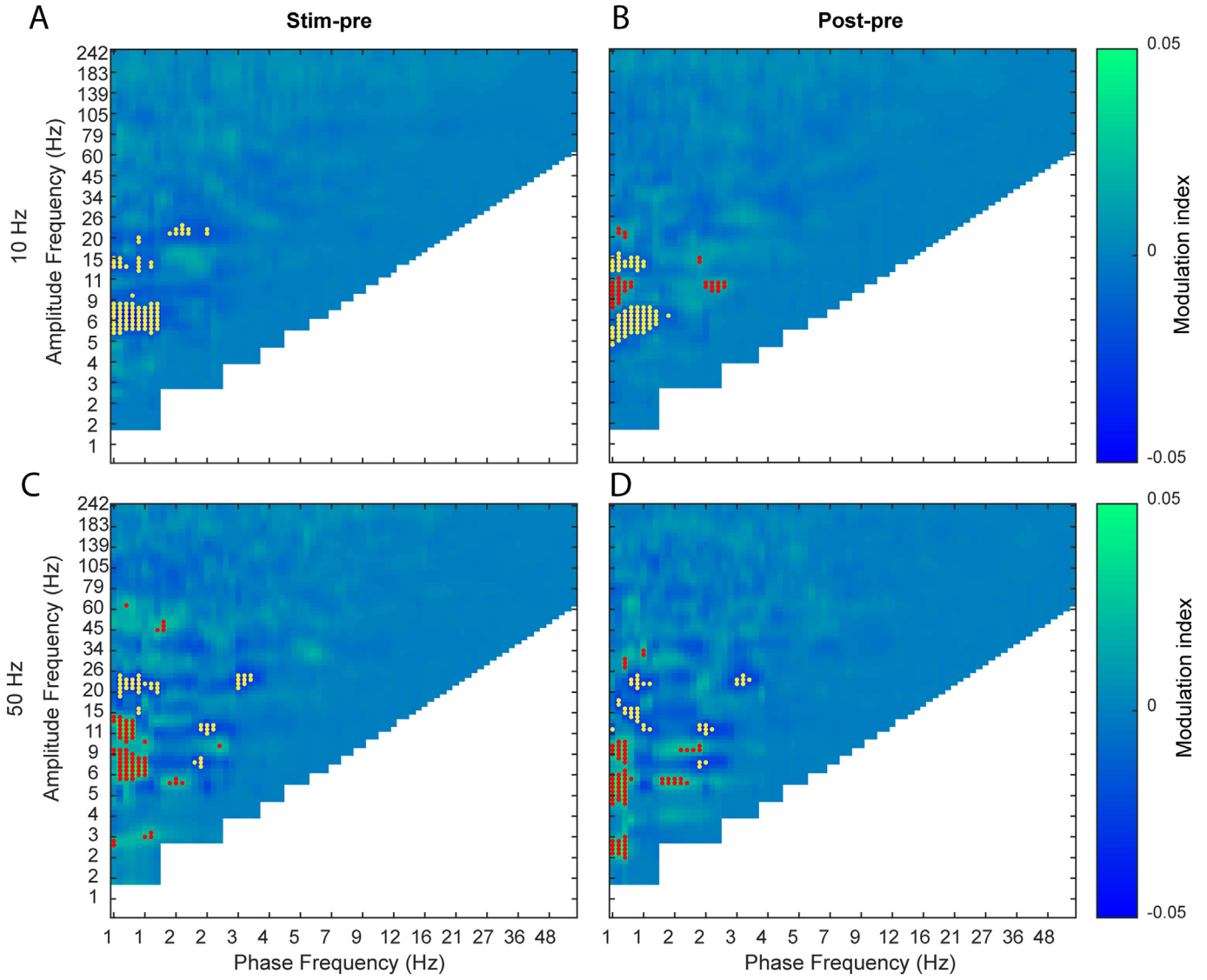

Fig. 4. Phase amplitude coupling within the seizure onset zone with 10 Hz and 50 Hz brain stimulation: (A) Stimulation with 10 Hz for 5 s induced reduced intra-hippocampal (SOZ) delta to theta/beta coupling during the stimulation (marked with yellow dots) as well as (B) increased (marked with red dots) delta to alpha coupling in the post-stimulation period increased (marked with red dots). (C) Stimulation with 50 Hz for 5 s on the other hand produced delta-theta/alpha coupling and decreased delta-beta coupling and (D) the response persisted in the post-stimulation window.

propagation of activation. Anatomical studies suggest topographic distinction within the medial-lateral dimension of the fornix with the anterior hippocampus occupying the lateral fornix, whereas the more medial fornix contains fibers from the septal/posterior hippocampus [24,25]. To our knowledge, this is the first electrophysiological study to demonstrate the asymmetric evoked responses in the anterior and posterior hippocampus highlighting the existence of a forniceal topography. Clinically, the asymmetric responses may be significant, given the functional differences between the anterior–posterior hippocampal axis [26]. Our study highlights that stimulation parameter, electrode configuration, and depth of implantation, all influence target engagement.

The crucial aspect of this study was how forniceal stimulation frequencies played a role in cortical activation and excitability. We ensured that all other stimulation parameters, i.e., current, pulse-width, and charge density, were kept constant except for the frequency, which was altered. We noted that high-frequency stimulation of a white matter tract resulted in an ictal response with a definitive increase in post-stimulation excitability within the SOZ and the limbic network. Low-frequency stimulation did not result in a seizure and showed reduced excitability in the post-stimulation window. Similar evidence was also reported by Koubeissi et al., where fornix was stimulated at 1 Hz stimulation over 4-h sessions (charge density: 20.13 $\mu C/cm^2$/phase). They show that hippocampal spiking significantly decreased, and the odds of seizure were reduced by 92% [2].

The electrode dimensions for the DBS at present are comparable to SEEG clinical macroelectrodes that exceed the fornix size. Therefore, LFPs recorded in bipolar derivation from two consecutive electrodes likely represent neural activity within and surrounding the fornix. Indeed, the PSD of the LFP demonstrated a theta bump suggesting the predominant inputs from the surrounding limbic structures. Sensing the field potentials offers the opportunity to develop closed-loop therapy and long-term monitoring of local changes in excitability and impedance. The latter function may be critical given the recent discoveries that degradation of axonal tracks, including the fornix, may set in early in neurodegenerative diseases like Alzheimer's disease [27].

A single case study, acute stimulation effects, the influence of anti-seizure medications, and the limited stimulation trials, all hinder the generalizability of the results. Despite such limitations, the case offers a significant insight that temporal patterning of forniceal stimulation affects target engagement at the local and network-level significantly.

Ethics statement

The study was approved by IRB, and written informed consent was obtained to perform research recording from deep brain structures such as the thalamus along with stimulation. Patients were explicitly informed about the risks associated with research implantation and our group has recently reported the consenting process, accuracy and safety of thalamic implantation.

Author contributions

SP was instrumental in the conception and design of the study, evaluation of the patient and EMU acquisition of data, contributed to data analysis and writing the manuscript. ET and GC performed analysis and interpretation of data and drafting the article and revising it critically for important intellectual content. KOR performed the robotic SEEG implantation. DP, LDI, TAM, KOR critically reviewed the manuscript, the analytical design and revised the manuscript critically for important intellectual content. SP in the capacity of the corresponding author agrees to be accountable for all aspects of the work in ensuring the accuracy or integrity of any part of the work investigated and resolved.

Declaration of competing interest

The authors declare that the research was conducted in the absence of any commercial or financial relationships that could be construed as a potential conflict of interest.

Acknowledgments

We would like to acknowledge the contributions of the patient, the family members, and UAB EMU EEG technicians towards achieving this study. SP, DP, TAM, LDI would like to acknowledge the continuous support from the USA National Science Foundation Grant (NSF RII-2 FEC OIA-1632891). SP and GC would also like to acknowledge support from NIH (1RF1MH117155-01).

References

[1] Girgis F, Miller JP. White matter stimulation for the treatment of epilepsy. Seizure 2016;37:28–31.
[2] Koubeissi MZ, Kahriman E, Syed TU, Miller J, Durand DM. Low-frequency electrical stimulation of a fiber tract in temporal lobe epilepsy. Ann Neurol 2013;74:223–31.
[3] Sweet JA, Eakin KC, Munyon CN, Miller JP. Improved learning and memory with theta-burst stimulation of the fornix in rat model of traumatic brain injury. Hippocampus 2014;24:1592–600.
[4] Miller JP, Sweet JA, Bailey CM, Munyon CN, Luders HO, Fastenau PS. Visual-spatial memory may be enhanced with theta burst deep brain stimulation of the fornix: a preliminary investigation with four cases. Brain 2015;138:1833–42.
[5] Ozdogmus O, Cavdar S, Ersoy Y, Ercan F, Uzun I. A preliminary study, using electron and light-microscopic methods, of axon numbers in the fornix in autopsies of patients with temporal lobe epilepsy. Anat Sci Int 2009;84:2–6.
[6] Leoutsakos JS, Yan H, Anderson WS, Asaad WF, Baltuch G, Burke A, et al. Deep brain stimulation targeting the fornix for mild Alzheimer dementia (the ADvance trial): a two year follow-up including results of delayed activation. J Alzheimers Dis 2018;64:597–606.
[7] Chaitanya G, Romeo A, Ilyas A, Irannejad A, Toth E, Elsayed G, et al. Robot-assisted stereoelectroencephalography exploration of the limbic thalamus in human focal epilepsy: implantation technique and complications in the first 24 patients. Neurosurgical focus; 2020 (Ahead of Print).
[8] Agnew WF, Yuen TG, McCreery DB. Morphologic changes after prolonged electrical stimulation of the cat's cortex at defined charge densities. Exp Neurol 1983;79:397–411.
[9] Cogan SF, Ludwig KA, Welle CG, Takmakov P. Tissue damage thresholds during therapeutic electrical stimulation. J Neural Eng 2016;13:021001.
[10] Avants BB, Tustison N, Song G. Advanced normalization tools (ANTS). Insight j 2009;2:1–35.
[11] Blenkmann AO, Phillips HN, Princich JP, Rowe JB, Bekinschtein TA, Muravchik CH, et al. iElectrodes: a comprehensive open-source toolbox for depth and subdural grid electrode localization. Front Neuroinform 2017;11:14.
[12] Brown CA, Johnson NF, Anderson-Mooney AJ, Jicha GA, Shaw LM, Trojanowski JQ, et al. Development, validation and application of a new fornix template for studies of aging and preclinical Alzheimer's disease. Neuroimage Clin 2017;13:106–15.
[13] Horn A, Li N, Dembek TA, Kappel A, Boulay C, Ewert S, et al. Lead-DBS v2: towards a comprehensive pipeline for deep brain stimulation imaging. Neuroimage 2019;184:293–316.
[14] Krauth A, Blanc R, Poveda A, Jeanmonod D, Morel A, Szekely G. A mean three-dimensional atlas of the human thalamus: generation from multiple histological data. Neuroimage 2010;49:2053–62.
[15] Pizarro D, Ilyas A, Chaitanya G, Toth E, Irannejad A, Romeo A, et al. Spectral organization of focal seizures within the thalamotemporal network. Ann Clin Transl Neurol 2019;6:1836–48.
[16] Toth E, Ganne C, Pati S. Mapping short-latency cortical responses to electrical stimulation of thalamic motor nuclei by increasing sampling rate-a technical report. Clinical Neurophysiology 2019.
[17] Alagapan S, Shin HW, Fröhlich F, Wu H-t. Diffusion geometry approach to efficiently remove electrical stimulation artifacts in intracranial electroencephalography. Journal of Neural Engineering 2018.
[18] Keller CJ, Honey CJ, Entz L, Bickel S, Groppe DM, Toth E, et al. Corticocortical evoked potentials reveal projectors and integrators in human brain networks. J Neurosci 2014;34:9152–63.
[19] Kardar M, Stella AL, Sartoni G, Derrida B. Unusual universality of branching interfaces in random media. Phys Rev E Stat Phys Plasmas Fluids Relat Interdiscip Topics 1995;52:R1269–72.
[20] Colombo MA, Napolitani M, Boly M, Gosseries O, Casarotto S, Rosanova M, et al. The spectral exponent of the resting EEG indexes the presence of consciousness during unresponsiveness induced by propofol, xenon, and ketamine. Neuroimage 2019;189:631–44.
[21] He BJ, Zempel JM, Snyder AZ, Raichle ME. The temporal structures and functional significance of scale-free brain activity. Neuron 2010;66:353–69.
[22] Tort AB, Komorowski R, Eichenbaum H, Kopell N. Measuring phase-amplitude coupling between neuronal oscillations of different frequencies. J Neurophysiol 2010;104:1195–210.

[23] Stypulkowski PH, Stanslaski SR, Giftakis JE. Modulation of hippocampal activity with fornix deep brain stimulation. Brain Stimul 2017;10:1125–32.
[24] Christiansen K, Metzler-Baddeley C, Parker GD, Muhlert N, Jones DK, Aggleton JP, et al. Topographic separation of fornical fibers associated with the anterior and posterior hippocampus in the human brain: an MRI-diffusion study. Brain Behav 2017; 7:e00604.
[25] Saunders RC, Aggleton JP. Origin and topography of fibers contributing to the fornix in macaque monkeys. Hippocampus 2007;17:396–411.
[26] Strange BA, Witter MP, Lein ES, Moser EI. Functional organization of the hippocampal longitudinal axis. Nat Rev Neurosci 2014;15:655–69.
[27] Ringman JM, O'Neill J, Geschwind D, Medina L, Apostolova LG, Rodriguez Y, et al. Diffusion tensor imaging in preclinical and presymptomatic carriers of familial Alzheimer's disease mutations. Brain 2007;130:1767–76.
[28] Rolls ET, Joliot M, Tzourio-Mazoyer N. Implementation of a new parcellation of the orbitofrontal cortex in the automated anatomical labeling atlas. Neuroimage 2015; 122:1–5.